19th Australasian Fluid Mechanics Conference
Melbourne, Australia
8-11 December 2014

Effect of Non-Axisymmetry in Arterial Stenoses

R. Padukkage[1] and T. Barber[1]

[1]School of Mechanical and Manufacturing Engineering
University of New South Wales, New South Wales 2052, Australia

Abstract

Atherosclerosis is the major cause of cardiovascular disease and hemodynamics is a crucial factor. Although statistics show that approximately 80% of occlusions are eccentric, models used in studies generally assume a symmetrically stenosed artery. While high shear stress is known to be atheroprotective, research has shown that low and oscillatory wall shear can lead to different types of plaque formation. We developed a model of an eccentric stenosed artery and compared the WSS distribution with an axisymmetric model. It was observed that the distribution of WSS was indeed different between the two models. This was at least in part due to the changes in the behaviour of the core jet flow and recirculation regions affected by the eccentricity of the stenosis.

Introduction

Atherosclerosis is commonly known as an inflammatory disease primarily characterized by internal thickening of an artery due to fibro-proliferative response resulting with a narrowed lumen [9] and hemodynamics is known to be a crucial contributor to this process. There are three known mechanical stresses induced by the blood flow that act on the vessel wall; blood pressure which acts perpendicular to the blood flow, cyclic stretch induced by pulsatile flow and shear stress [2]. Wall shear stress (WSS) refers to the frictional drag force that acts on the vessel wall parallel to the blood flow [1]. This drag force is then mechanotransduced into chemical signals that can be understood by vascular cells in order to maintain regular vascular behaviour [8]. CFD simulations conducted to study the effect of a stenosis on the resulting variations in wall shear stress distribution often assume a symmetric occlusion. However research shows that the majority of physiological occlusions are eccentric [4]. The main aim of this study was to compare the effects of differently shaped stenosis; axisymmetric and eccentric, on blood flow. The axisymmetric model was based on the stenosis profile developed by Siouffi et al. [11] while a more physiological, eccentric model was created based on histological cross-sections of stenosed arteries (see Figure 1 and Figure 2).

Axisymmetric and eccentric stenosed artery CFD models were constructed while maintaining a constant occlusion level. This ensured that eccentricity would be the only factor that contributes to the differences in flow behaviour if any are observed. The physiological triphasic velocity profile of a femoral artery was used as the inlet function. Since WSS is directly proportional to velocity, data obtained from the simulations were used to generate vector fields and velocity profiles at the mid plane as well as colour contours of cross sections. This information was then used to understand the flow behaviour that contributed to the differences observed in oscillatory shear index (OSI) distribution.

Method

To construct the computational model, the common femoral artery was used since arteries with a larger diameter are more susceptible to WSS and hence more vulnerable to atherogenesis. The dimensions for the model were adapted from an adult human male. The non-occluded regions of the artery for both models were assumed circular with a uniform diameter of 10 mm throughout the 400 mm length. The occluded cross-section was placed at the centre of the geometry (length wise) so that there was sufficient length for the fluid to develop by the time it reached the area of concern. ANSYS ICEM CFD 14.5 was used as the computational software to generate a structured hexahedral mesh (Figure 3).

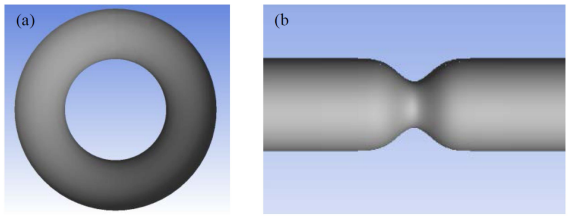

Figure 1: The geometry of the axisymmetric stenosed model. a) Cross section. b) Side view.

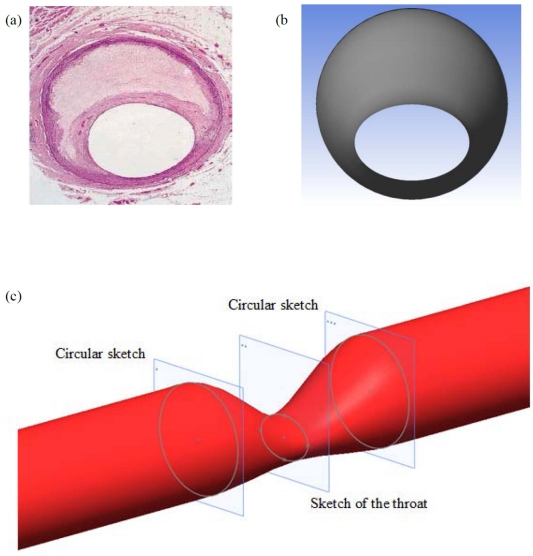

Figure 2: The geometry of the eccentric stenosed model. a) Histological cross section (Adapted from [10]). b) Cross section of the 3D model. c) Isometric view with the three planes used to construct the 3D model.

Though blood is considered to be a non-Newtonian fluid, for the convenience of this study the fluid was assumed a Newtonian fluid. The graph in Figure 4 represents the physiological cardiac cycle of the femoral artery that was used in this study. Five different time points with different velocities were taken into consideration and can be identified by the red dots. With a maximum Re value of 1884 at the inlet and a much higher ex-

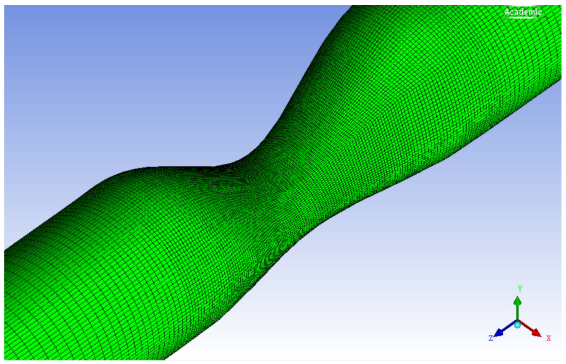

Figure 3: Isometric view of the refined mesh.

pected value at the occlusion, it was certain that the flow tend to be more erratic compared to a laminar flow behaviour; therefore turbulence modelling was preferred. The shear Stress Transport (SST) K-ω turbulence model was used for turbulence closure. A density of 1060 kgm^{-3} and a constant dynamic viscosity of 0.0035 $kgs^{-1}m^{-1}$ were assumed. All terms were solved with second order accuracy. A target residual value of 10^{-5} was adapted in order to maximise the accuracy of results as well as minimise computational time. The mesh was refined until both values of WSS and maximum velocity, had minimal changes between consequently refinements. Four consecutive refinements were made for each geometry and the key parameters were obtained for each mesh. The test revealed that the key parameters remained almost constant after the third refinement which had an element count of 1.7 million. A grid convergence for the eccentric stenosed geometry was reached by the third refinement and it contained 1.6 million elements. With the intention of analyzing a constant oscillatory motion of blood flow the fifth cardiac cycle was utilized to obtain the CFD results.

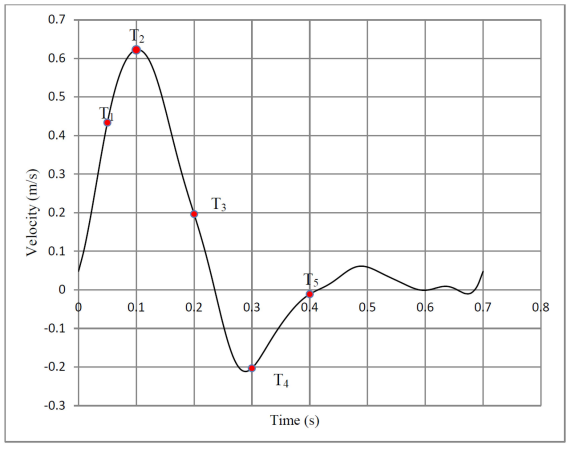

Figure 4: Physiological velocity profile of a femoral artery.

Results

To understand the fluid flow behaviour, vector fields along the mid plane were generated. The recirculation regions are denoted by R and the low velocity regions by LV. At T-1, the mid-plane vector plot shown in Figure 5, displays the prominent recirculation areas for both models. For the eccentric model, recirculation regions were observed near the top wall and at the bottom edge of the high velocity stream. When the inlet velocity reaches a negative value (Figure 5), the flow was reversed and the vector plots appeared to be a mirror image of the results obtained at the first time point. The only other difference was that the eccentric model displayed a low velocity region towards the bottom wall proximal to the throat.

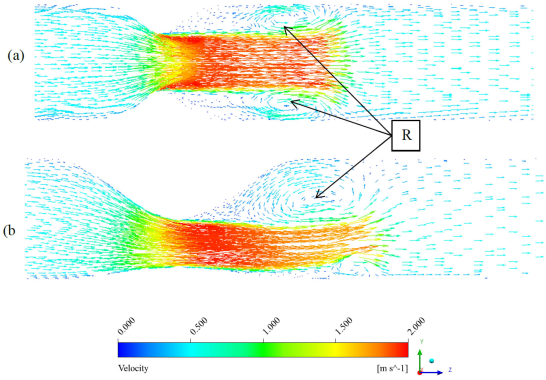

Figure 5: Vector fields plots at T-1. a) axisymmetric model. b) Eccentric model.

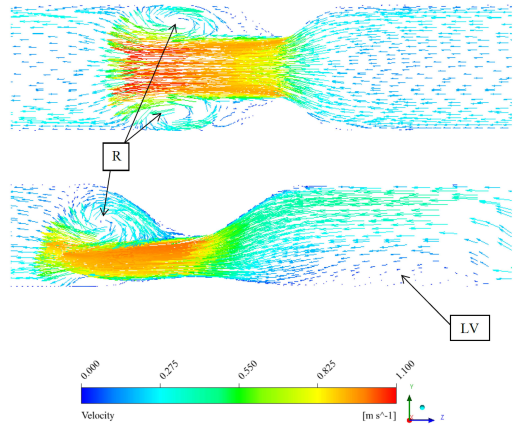

Figure 6: Vector fields plots at T-4. a) axisymmetric model. b) Eccentric model.

Since it was of interest to determine the effect of occlusion eccentricity on WSS distribution, contour plots were utilised to compare the two models at different time points. A local scale applicable to both models was used to visualise the full spectrum of WSS in order to accommodate the comparison. For positive velocities, most of the variations in WSS were only observed after the throat in both models. By the first time point (Figure 7), the eccentric model showed a gradual increase in WSS before the throat while a sudden increase was noticed for the axisymmetric model. The maximum WSS for both models were recorded at the proximal region of the plaque which is consistent with previous studies [5]. However, a magnitude discrepancy of 40 Pa was observed between the two models, where the axisymmetric model displayed the higher value over the eccentric model. As the inlet flow reverses (Figure 8), the regions of interest shift from downstream to upstream. At T-4, the maximum WSS values were 38 Pa and 26 Pa respectively for the axisymmetric and the eccentric models. These were observed again at the throat however on the downstream region of the occlusion. In addition, a distinct peak can be seen 10 mm upstream of the axisymmetric model. In contrast, fluctuation in WSS distribution around the occlusion was observed for the eccentric model which evened out 80 mm after and 30 mm before the throat. Whereas the WSS values of the axisymmetric model became constant 10 mm after and 20 mm before the throat.

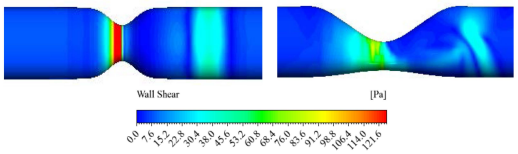

Figure 7: WSS contour plot with a global colour map for T-1 a) axisymmetric model b) eccentric model.

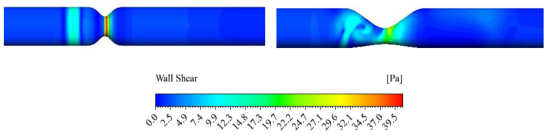

Figure 8: WSS contour plot with a global colour map for T-4 a) axisymmetric model b) eccentric model.

Time averaged WSS was considered to capture the significant differences between the two models. This analysis was carried out using OSI formulated by He et al. [3] which represents the fluctuation in wall shear. The OSI function was incorporated into ANSYS Fluent as a user defined function (UDF) and the index value zero represents the lowest oscillatory wall shear and 0.5 represents the highest oscillatory wall shear stress. The results obtained by this OSI function are shown in Figure 9a and Figure 9b for the axisymmetric and eccentric models respectively.

It was observed that the OSI distribution was completely different between the two models. The axisymmetric model showed a more symmetric OSI distribution with the highest oscillation proximal to the throat and also four to five diameters further downstream Figure 9a. The lowest OSI value was observed just before the throat indicating minimal variation in wall shear throughout the cycle.

In the eccentric model, the OSI distribution appeared to be more random with a prominent low OSI region near the bottom wall proximal to the throat Figure 9b. The other distinct noticeable difference was on the side walls where it showed a unique line of high OSI which propagated downstream.

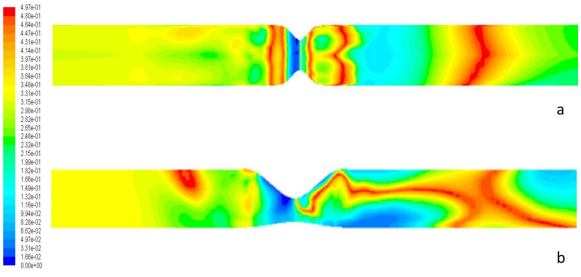

Figure 9: OSI distribution. a) axisymmetric model. b) eccentric model.

Discussion

It was evident from the contours that the distribution of wall shear and oscillatory wall shear stress depends on the eccentricity of stenosis. The spread of regions experiencing high, low and oscillatory WSS were unique to each model where the distributions were more symmetric for the axisymmetric model and irregular for the eccentric model. However at the throat, both models showed the highest magnitude of WSS and less or no presence of oscillation. While both low and oscillating wall shear are known to be crucial for atherogenesis, research by Cheng et al. [1] has shown that areas prone to oscillatory shear stress are likely to induce formation of more stable plaques that are less prone to rupture. Low shear stress induces plaques that are larger in size and with a necrotic core although with less lipid content and a thinner fibrous cap. Hence it is evident that if only an axisymmetric model is considered when analysing the areas that are vulnerable to the effects of an already existing stenosis, the decisions are likely to be more biased. At the same time, relatively high levels of WSS are thought to be atheroprotective. However, if the stress level is above a certain level (40 Pa), it can result with adverse affects such as rupture of the atherosclerotic plaque. Hence determining the WSS at throat is important. It was observed that the axisymmetric model resulted with a higher magnitude at the throat over the eccentric model. Therefore it is necessary to choose a model that more closely represents the physiological state to avoid over or under estimation of WSS.

To understand the differences between the two OSI contours (Figure 10A and 10B), both mid plane velocity vector fields (Figure 10C and 10D) and contours (Figure 10E and 10F) were considered. To construct these contours, cross sectional velocity contours were incorporated with mid plane contours and are displayed from an isometric view. For convenience, only the velocity vector fields and contours obtained at the positive peak velocity are show.

The main two aspects that contributed towards the changes in velocity variance were the main fluid jet flow (high velocity regions) and the recirculation areas (low velocity regions). Since WSS is proportionate to the velocity gradient, the differences in WSS and OSI observed between the two models are predominantly due to aforementioned two aspects.

In the eccentric model, the main fluid jet travels in the form of a wave after exiting the throat. The area in the bottom wall where the jet initially hits (black circle) experiences constant high velocity in the same direction throughout majority of the cycle (Figure 10C and shown elsewhere). Hence this particular region is not exposed to significant fluctuations in WSS and thus assigned a low OSI (black circle, Figure 10A). Moreover this significant wave shaped jet present throughout majority of the cycle, gives rise to a constant surface of separation creating a continuous recirculation region towards the upper wall (R1 in Figure 10C). Thus resulting with a constant low velocity region which experience low oscillatory wall shear as denoted with black arrows in Figure 10A.

The point where the wake hits the upper wall causes the surface of separation to reattach creating a zero velocity region. However, as the reattachment length fluctuates according to the inlet velocity, the point of reattachment varies resulting with a rapidly changing velocity region. This gives rise to the high OSI observed in the upper wall within the red square in Figure 10A. As the fluid jet proceeds and touches the bottom wall further downstream, it creates another recirculation region (R2 C, Figure 10) with another reattachment point which also fluctuates with time contributing to the high OSI region at the bottom wall. During the cardiac cycle, the characteristics within the region denoted by the red square oscillate perpendicular to the centre axis with time. This change might have caused the spread of high OSI region observed throughout the wall in this region. When looking at the isometric view in Figure 10E, it also shows that the high velocity regions disperse throughout the downstream wall. In contrast, in the axisymmetric model, the only significant observation was the high OSI region within the green square. This is a consequence of the fluctuation of the

reattachment point. Since the recirculation zones are symmetric and due to the symmetry of the throat, the high OSI region is observed all around the wall. To better understand the fine details observed in OSI distribution, additional contours of cross sections along the model and time averaged WSS contours would be required of both models.

While both low WSS and high OSI are reported to coincide with subsequent stenosis formation [6], it is suggested that OSI is a better predictor of further development of stenosis [7]. In addition, research has shown that regions experiencing high OSI values are prone to develop atherosclerotic plaques that are more stable with a thick fibrous cap [1]. When looking at the results, it is evident that flow behaviour, WSS distribution and OSI distribution are quite different between an axisymmetric and eccentric model. Furthermore, the area observed to experience high OSI was much larger in the eccentric model compared to the axisymmetric model. Hence when recruiting CFD analysis to determine the regions that are more susceptible to subsequent stenoses, it is unwise to assume complete symmetry of the occlusion.

A limitation of the study was the fact that CFD analysis does not accommodate for the dynamics factors within the blood vessel. The vessel wall was assumed to be rigid during the simulation. This does not account for the visco-elastic nature of the blood vessel which to a certain extent can accommodate for the shear stress exerted by the blood flow by altering the size of the lumen. We cannot predict if under physiological conditions, given the extremity of the occlusion, blood pressure and observed shear stress exerted on it, whether the plaque would already rupture. Buffering effect from the dynamic vessel wall hence is overlooked.

We aimed to develop and simulate a more physiological model of a stenosis. However, for ease of modelling, we assumed the diameter of the vessel to be uniform throughout the length which is not physiologically true. We also assumed blood to be a Newtonian fluid while over-looking the non-Newtonian properties that might have altered the shear stress exerted on the walls to a certain extent.

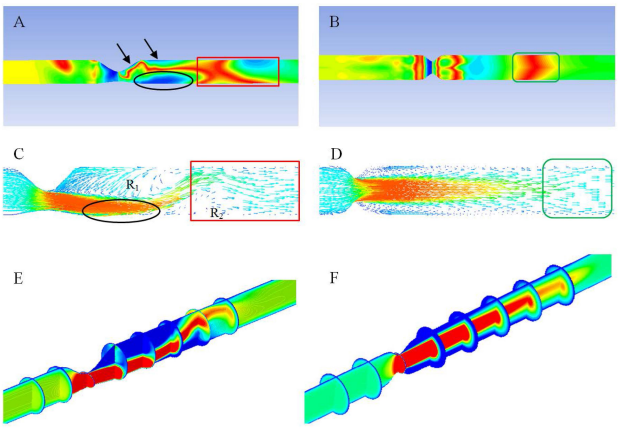

Figure 10: OSI contour for a) Eccentric model b) Axisymmetric model. Velocity vector fields at T-2 for c) eccentric model d) axisymmetric model. Combination of mid plane and cross sectional velocity contours for e) eccentric model f) axisymmetric model.

Conclusions

This study presented a comparison between an axisymmetric stenosed model and an eccentric model in terms of WSS distribution and OSI. We observed that distribution of WSS and OSI was significantly different, both in terms of magnitude and localisation, between the two models. This was at least in part due to the effect of stenosis eccentricity on the behaviour of fluid jet stream and recirculation regions. Although data obtained for low WSS was not sufficient enough to draw insightful conclusions, we were able to successfully compare the two models using high WSS and OSI distribution. Thus we conclude that when performing CFD simulation to determine the regions that are more susceptible to subsequent stenoses, it is unwise to assume complete symmetry of the occlusion.

References

[1] Cheng, C., Tempel, D., van Haperen, R., de Boer, H. C., Segers, D., Huisman, M., van Zonneveld, A. J., Leenen, P. J., van der Steen, A., Serruys, P. W. et al., Shear stress–induced changes in atherosclerotic plaque composition are modulated by chemokines, *The Journal of clinical investigation*, **117**, 2007, 616–626.

[2] Cunningham, K. S. and Gotlieb, A. I., The role of shear stress in the pathogenesis of atherosclerosis, *Laboratory investigation*, **85**, 2004, 9–23.

[3] He, X. and Ku, D. N., Pulsatile flow in the human left coronary artery bifurcation: average conditions, *Journal of biomechanical engineering*, **118**, 1996, 74–82.

[4] Insull Jr, W., The pathology of atherosclerosis: plaque development and plaque responses to medical treatment, *The American journal of medicine*, **122**, 2009, S3–S14.

[5] Lovett, J. K. and Rothwell, P. M., Site of carotid plaque ulceration in relation to direction of blood flow: an angiographic and pathological study, *Cerebrovascular Diseases*, **16**, 2003, 369–375.

[6] Olgac, U., Poulikakos, D., Saur, S. C., Alkadhi, H. and Kurtcuoglu, V., Patient-specific three-dimensional simulation of ldl accumulation in a human left coronary artery in its healthy and atherosclerotic states, *American Journal of Physiology-Heart and Circulatory Physiology*, **296**, 2009, H1969–H1982.

[7] Peiffer, V., Sherwin, S. J. and Weinberg, P. D., Does low and oscillatory wall shear stress correlate spatially with early atherosclerosis? a systematic review, *Cardiovascular research*, cvt044.

[8] Resnick, N., Yahav, H., Shay-Salit, A., Shushy, M., Schubert, S., Zilberman, L. C. M. and Wofovitz, E., Fluid shear stress and the vascular endothelium: for better and for worse, *Progress in biophysics and molecular biology*, **81**, 2003, 177–199.

[9] Ross, R., Rous-whipple award lecture. atherosclerosis: a defense mechanism gone awry., *The American journal of pathology*, **143**, 1993, 987.

[10] Sambola, A., Fuster, V. and Badimon, J. J., Role of coronary risk factors in blood thrombogenicity and acute coronary syndromes, *Revista espanola de cardiologia*, **56**, 2003, 1001–1009.

[11] Siouffi, M., Pelissier, R., Farahifar, D. and Rieu, R., The effect of unsteadiness on the flow through stenoses and bifurcations, *Journal of biomechanics*, **17**, 1984, 299–315.